Mon. Not. R. Astron. Soc. **359,** L23–L26 (2005) doi:10.1111/j.1745-3933.2005.00027.x

Beating the Poisson limit by coupling an occulting mask to wavefront sensing

Brice Le Roux★ and Roberto Ragazzoni

Osservatorio Astrofisico di Arcetri (INAF), Largo E. Fermi 5, 55125 Firenze, Italy

Accepted 2005 February 1. Received 2005 February 1; in original form 2005 January 11

ABSTRACT

We show that by coupling an occulting mask to a wavefront sensor one can achieve sensitivities that exceed by a factor of 2 in variance the Poissonian limit in wavefront sensing. Examples of applications are the extension to fainter objects of conventional adaptive optics, and the increase in the sky coverage of natural guide star multiconjugated adaptive optics.

Key words: instrumentation: adaptive optics.

1 INTRODUCTION

The wavefront sensor (WFS) is a key element of an adaptive optics (AO) system. It gives access to a direct measurement of the turbulent phase, its curvature or its slope (Shack–Hartmann or pyramid wavefront sensors), from which the mirror voltages are computed. The ability of the system to correct efficiently the atmospheric turbulence is strongly dependent on the performance of the WFS in estimating the turbulent phase. The Shack–Hartmann (SH) WFS (Shack & Platt 1971) has been for a long time the standard used in AO systems. Its limits have been studied and thought to be almost unbeatable (Angel 1994; Rousset 1999). In 1995 a new generation WFS, the pyramid WFS, was proposed (Ragazzoni 1996). It is a focal-plane WFS, based on the principle of a Foucault knife-edge. It has been demonstrated that it provides a consistent gain with respect to the SH WFS (Ragazzoni & Farinato 1999; Esposito & Riccardi 2001; Vérinaud 2004). More recently, efforts have been made to increase the SH WFS performance (Poyneer & Macintosh 2003; Nicole et al. 2004; Le Roux, Coyne & Ragazzoni 2005) and to compare the pyramid with the SH (Vérinaud 2005), in view of new systems which need improvements in wavefront sensing, such as extreme AO (XAO) systems for exo-planet searches (Flicker 2003; Feldt et al. 2003) or multiconjugated AO (MCAO) systems (Beckers 1988; Hubin et al. 2001) for a large field of view with high resolution.

Coupling an occulting mask and a WFS to achieve an even further improvement of the wavefront sensing performance has been proposed by Ragazzoni (2003). In this Letter, we explain in detail why this technique improves the wavefront sensing, and we give first quantitative estimates of the gain obtained.

2 PRINCIPLE AND GEOMETRICAL APPROXIMATION

We propose in this Letter to study the effect on the wavefront sensing of an occulting mask placed on a focal plane before the WFS. We give in this section a physical understanding of the concept in the case of a four-quadrant WFS. We will generalize this to the pyramid WFS with numerical simulations in Section 3. The concept is represented in Fig. 1. On the left-hand side of the figure is drawn a four-quadrant which is placed on the focal plane and on to which an image is focused. The WFS measurement is given by the difference of illumination on each of the four quadrants. On the right-hand side of the figure is represented the same WFS plus a mask at its centre. The centre of the image is cut by the mask.

To illustrate and explain physically why one can expect that this configuration should bring a certain gain, let us consider the estimation of a pure tilt with the four-quadrant WFS. Represented in Fig. 2 are the four quadrants in the focal plane, showing images with and without tilt in the turbulent phase, with and without the mask (respectively left- and right-hand parts of Fig. 2). The effect of the tilt is a displacement of the image, a pure translation. The estimation of the value of the tilt by the WFS corresponds to the estimation of the amplitude of this displacement. In the figure, the displacement is much smaller than the image size. In that configuration, what allows the estimation of the displacement of the spot is essentially the disappearance of photons on the left-hand side and the appearance of other photons on the right-hand side. If someone had access only to a little window centred on the centre of the four-quadrant, the appearance or disappearance of photons could not be seen, only photon noise would be measured, and the estimation of tilt would be impossible. This leads us to the conclusion that some photons are not bringing any information useful for the estimation of the tilt, but are only bringing noise, through the Poissonian fluctuation of such light. The noise brought by those photons is comparable to the background light photons. One could in fact consider that the presence of 'not useful' photons in the centre of the field consists, in practice, of an increase in the background noise. In Fig. 2, we represent the zone corresponding to the 'not useful' photons in dark grey and the zone corresponding to the 'useful' photons in light grey. We place in the right-hand part of the figure a mask which is inside the 'not useful' zone, blocking the photons that do not give any information but do bring noise. One can then already understand in this geometrical approximation why a gain is expected.

★E-mail: leroux@arcetri.astro.it

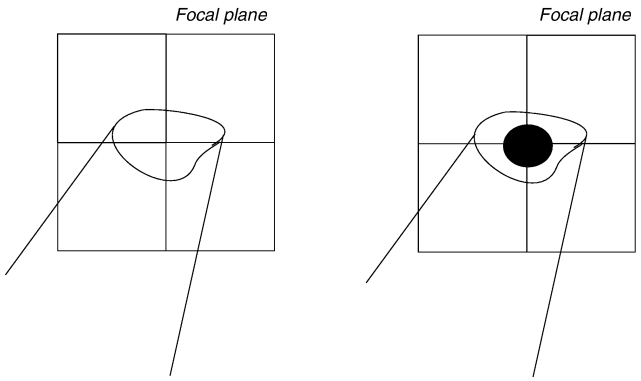

Figure 1. Principle of the occulting mask WFS. A mask is placed in front of a focal-plane WFS.

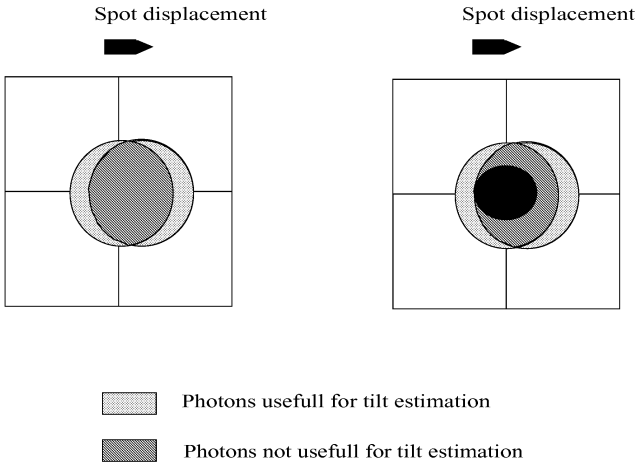

Figure 2. Illustration of the physical origin of the gain provided by the occulting mask WFS, in the simple case of a tilt and a four-quadrant WFS.

Fig. 3 explores more quantitatively the effect of the occulting mask. $N_{\rm ph}$ is the number of photons arriving on each quadrant when the spot is centred and without the mask. $N_{\rm ph}$ is the number of photons arriving on each quadrant when the spot is centred with the mask. In the tilt case, the number of photons passing from left-hand quadrants to right-hand quadrants is the same with and without the mask: X. The estimation of the tilt is directly linked to the number of photons X. The ability to estimate X depends on the ratio between X and the photon noise variance, and this is much lower in the mask case. The expected gain of a WFS coupled with a mask is then clearly to be found in the sensitivity of the measurement to the photon noise. We present in Fig. 4 the illustration of this behaviour. Owing to the Poisson nature of the photon noise, the number of photons is fluctuating with time. We call 'noise realization' the number of photons at a given instant. When the noise realization changes, the estimated slopes change too. The expected variance of all the measurements for a given perturbation is plotted. For a fixed perturbation, measured several times with several photon noise realizations, the variance of the measurement provided by a mask coupled with a WFS should be smaller than the variance of the measurement of the single WFS.

Moreover, it is also possible to predict the behaviour of the optimal size of the mask. It is clear in the illustration drawn in Fig. 5 that it

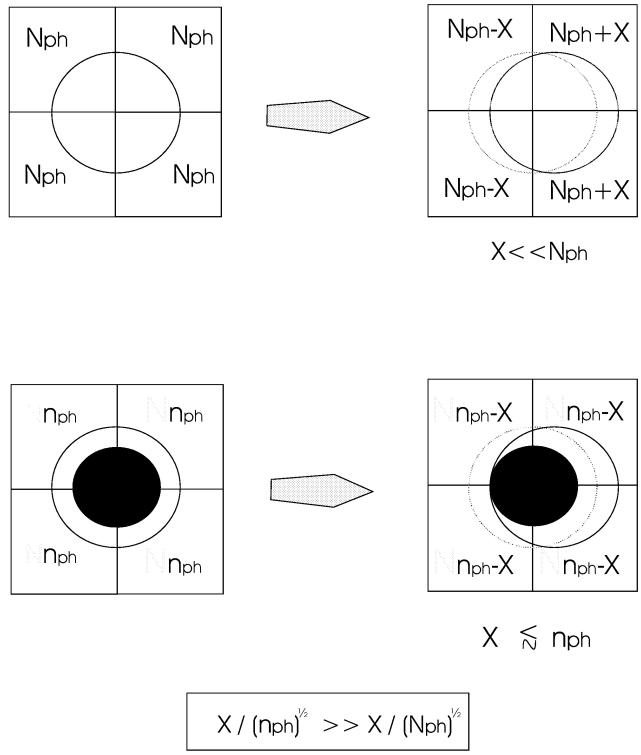

Figure 3. An occulting mask WFS approach allows a better sensitivity. The number of photons X that appear or disappear from a quadrant is the quantity linked to the tilt estimation.

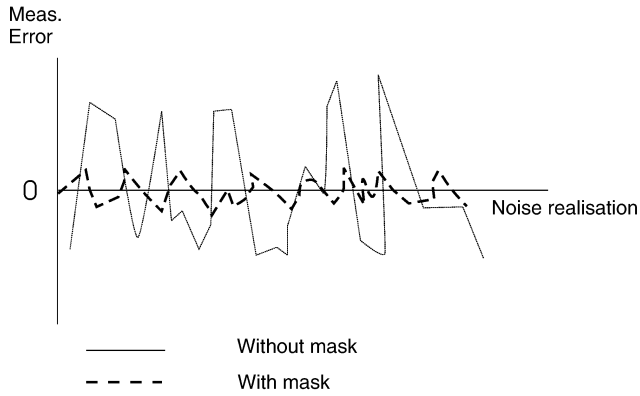

Figure 4. Illustration of the expected behaviour of an occulting mask WFS and of a 'classical' WFS with respect to the noise realizations. The mask tends to limit the variance of the measurement.

depends on the Fried parameter r_0. The larger r_0, the larger the mask. If the displacement is very small (the case of very low turbulence), one can predict that the optimal mask size is quasi-equal to the image size. That means that in a closed loop (the case of very low turbulence on the WFS), one can expect that the optimal size of the mask would not be far from λ/D, where λ is the wavelength and D the telescope diameter.

Of course, all this physical understanding of the phenomena has been made in geometrical optics and needs to be validated in a real case, which means taking into account the diffraction effects. We explore this by numerical simulations in the next section.

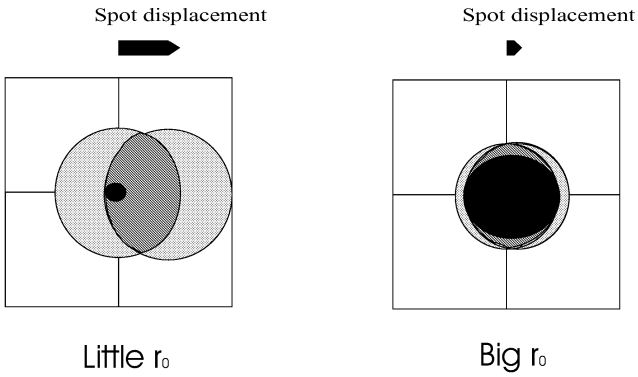

Figure 5. The optimal size of the mask depends on the turbulence strength. The stronger the turbulence (the smaller r_0), the smaller the mask.

3 VALIDATION IN THE DIFFRACTIVE CASE BY NUMERICAL SIMULATIONS

We present in this section numerical simulations that demonstrate the validity of the occulting mask wavefront sensing concept in the diffractive case, to verify the predictions made previously in geometrical optics and to quantify the gain of the approach that we propose with a pyramid WFS. The results obtained here are first results. They should be completed later by a more precise and full closed-loop study.

3.1 Simulation tools and simulation conditions

We first simulated open-loop turbulence screens with the Mc Glamery method (Mac Glamery 1976). This approach allows us to impose the spectrum of the turbulence by passing by the Fourier space. We chose to simulate turbulence based on Kolmogorov statistics.

We then simulated a pyramid WFS without a mask. The pyramid WFS gives four images of the pupil, each of them corresponding to one quadrant. To compute each image we created an amplitude filter which was transparent only on the considered quadrant and opaque everywhere else. Each image is given by

$$\boldsymbol{I}_i = \mathrm{FT}[|\mathrm{Filt}_i * \mathrm{FT}(\mathrm{e}^{-\mathrm{i}\phi})|^2], \quad (1)$$

where ϕ corresponds to the phase screen, FT denotes the Fourier transform and Filt_i is the filter which is transparent for quadrant i. For illustration we present in Fig. 6 (left) the filter corresponding to quadrant 1.

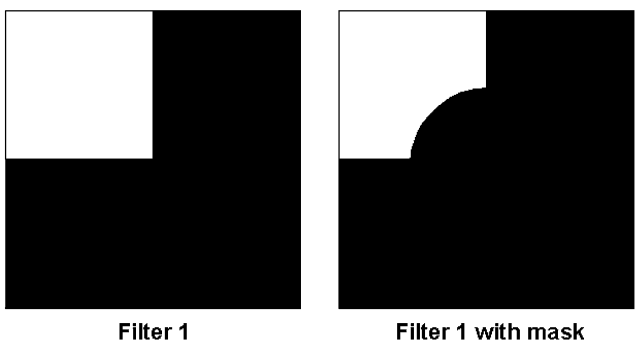

Figure 6. Illustration of the filters corresponding to quadrant 1 in the cases with and without a mask.

The photon noise is introduced by creating a Poisson noise realization with mean $\boldsymbol{I}_i$:

$$I_i = \mathrm{Poisson}(|\boldsymbol{I}_i|). \quad (2)$$

From the four images I_1, I_2, I_3, I_4 behind the pyramid, one can extract the phase slope estimates:

$$S_x = [(I_1 + I_2) - (I_3 + I_4)],$$
$$S_y = [(I_1 + I_4) - (I_2 + I_3)]. \quad (3)$$

Next, we added the mask to the simulation. The only change appears in the creation of the filters. The mask corresponds to a central disc added to the previous filters. We represent for illustration in Fig. 6 (right) the filter corresponding to quadrant 1 with a mask.

In both cases with and without a mask we computed the variance of the measurement error. The error was computed by comparing the slope measurement with the exact values obtained on the phase screen itself. We computed the error given by the WFSs with 100 photon noise realizations and 100 turbulence realizations, for the given r_0. The best mask size d_{mask} was fixed by minimizing numerically the variance of the error of estimation as a function of d_{mask}.

In the simulation, we chose $r_0 = D$. It corresponds to a 'closed loop-like' case, meaning a case with very small perturbations. In doing this, we were able to verify the behaviour expected and predicted in the previous sections.

3.2 Results and interpretation

We obtain results that agree closely with the physical understanding of the phenomena presented in Section 2. Fig. 7 presents the variance of the slope estimation error as a function of the signal-to-noise ratio (SNR). The SNR is here defined as the square root of the mean number of photons. The mask size has been optimized for each SNR, and we find that the best d_{mask} is not dependent upon the SNR and $d_{\mathrm{mask}} = \lambda/D$.

We observe in the figure that the mask coupled with the WFS decreases the variance representing the sensitivity to photon noise by a factor of 2. The gain is obviously much bigger in absolute value for a low SNR than for a high SNR.

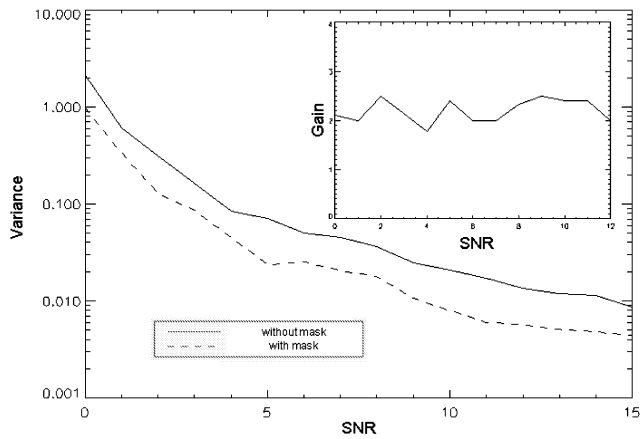

Figure 7. Behaviour of the variance of measurement error as a function of SNR with and without a mask. We obtain a gain in variance of a factor of 2.

4 CONCLUSION

We have shown that a mask coupled with a WFS results in an increase of the sensitivity of the WFS by a factor of 2 in variance, as long as the mask size is optimized properly.

The results have practical applications in every AO system looking at faint stars, and in natural guide star-based MCAO systems, which need to have access to faint stars to extend the sky coverage. From the results we have obtained, one can deduce that the limiting magnitude is increased by 1.5 and therefore the sky coverage is increased by a factor of between 2 and 4, depending on the position on the sky.

XAO systems for planet finder-like projects today investigate cases of AO in bright stars in order to be able to sample spatially the wavefront enough to have access to the very high frequencies of the turbulence. This means in practice many pixels on the CCD camera behind the pyramid and then a low number of photons on each pixel. XAO systems, in that sense, have access to a low flux and high photon noise in the WFS process, and could therefore take good advantage of the coupling of an occulting mask and WFS.

ACKNOWLEDGMENTS

This work has been partially funded by the European Research and Training Network Adaptive Optics for Extremely Large Telescopes, Contract HPRN-CT-2000-00147.

REFERENCES

Angel J. R. P., 1994, in Alloin D. M., Mariotti J.-M., eds, NATO Series C, Adaptive Optics for Astronomy. Kluwer, Dordrecht, p. 139
Beckers J., 1988, in Ulrich M.-H., ed., Very Large Telescopes and their Instrumentation, Vol. 2. ESO, Garching, p. 693
Esposito S., Riccardi A., 2001, A&A, 372, 710
Feldt M. et al., 2003, in Schultz A. B., ed., Proc. SPIE Vol. 4860, High contrast imaging for Exo-planet detection. SPIE, Bellingham, p. 149
Flicker R. C., 2003, A&A, 405, 1177
Hubin N. et al., 2001, in Vernet E., Ragazzoni R., eds, ESO Conf. Workshop Proc. Vol. 58, Beyond conventional Adaptive Optics. ESO, Garching, p. 27
Le Roux B., Coyne J., Ragazzoni R., 2005, Appl. Opt., 44, 10
Mac Glamery B., 1976, Image Processing, 74, 225
Nicole M., Fusco T., Rousset G., Michau V., 2004, Opt. Lett., 29, 2743
Poyneer L. A., Macintosh B. A., 2003, in Tyson R. K., Lloyd-Hart M., eds, Proc. SPIE Vol. 5169, Astronomical AO systems and applications. SPIE, Bellingham, p. 190
Ragazzoni R., 1996, J. Mod. Opt., 43, 289
Ragazzoni R., 2003, in Ardeberg A. L., Andersen T., eds, Proc. SPIE Vol. 5382, Extremely Large Telescopes. SPIE, Bellingham, p. 456
Ragazzoni R., Farinato J., 1999, A&A, 350, L23
Rousset G., 1999, in Roddier F., ed., Adaptive Optics in Astronomy, ch. 5. Cambridge Univ. Press, Cambridge, p. 91
Shack R. B., Platt B. C., 1971, J. Opt. Soc. Am., 61, 656
Vérinaud C., 2004, Opt. Commun., 233, 27
Vérinaud C., 2005, MNRAS, 357, L26

This paper has been typeset from a TEX/LATEX file prepared by the author.